Chemical structure of the ultrathin SiO_2/Si(100) interface: An angle-resolved Si 2*p* photoemission study

J. H. Oh
Department of Applied Chemistry, The University of Tokyo, 7-3-1 Hongo, Bunkyo-ku, Tokyo 113-8656, Japan

H. W. Yeom*
Atomic-scale Surface Science Research Center and Institute of Physics and Applied Physics, Yonsei University, Seoul 120-749, Korea

Y. Hagimoto, K. Ono, and M. Oshima
Department of Applied Chemistry, The University of Tokyo, 7-3-1 Hongo, Bunkyo-ku, Tokyo 113-8656, Japan

N. Hirashita, M. Nywa, and A. Toriumi
STARC, Shimbasi 6-16-10, Minato-ku, Tokyo 105-0004, Japan

A. Kakizaki
Institute of Materials Structure Science, High Energy Accelerator Research Organization, Oho 1-1, Tsukuba 305-0801, Japan
(Received 11 September 2000; revised manuscript received 16 January 2001; published 24 April 2001)

The ultrathin SiO_2/Si(100) interface has been investigated by extensive high-resolution angle-resolved photoemission measurements of the Si 2*p* core levels. The polar angle dependence of the Si 2*p* intensities are measured in detail for the different suboxide (Si^{1+}, Si^{2+}, and Si^{3+}) components originating from transition layers at the interface. The depth distribution of the different suboxide species is quantitatively analyzed by a simple electron attenuation scheme. It is unambiguously shown that the Si^{3+} species is distributed over a significantly wider region from the interface, while the Si^{1+} and Si^{2+} species exist mostly within the first interfacial layer. A chemically nonabrupt interface is thus clearly supported, and a simple interface model is introduced which is composed of three transition layers.

DOI: 10.1103/PhysRevB.63.205310 PACS number(s): 68.35.Ct, 79.60.Jv

I. INTRODUCTION

State-of-the-art device technology demands the reduction of gate-oxide film thickness down to as thin as 1 nm where the chemical abruptness of the SiO_2/Si interface largely affects the performance of a silicon device.[1,2] Thus it is, of crucial technological importance to understand the structure and the chemical abruptness of the SiO_2/Si interface.[3] However, an atomic-scale understanding of the interface structure and chemistry is still lacking, with the fundamental difficulty of connecting the amorphous SiO_2 with a crystalline silicon surface in atomic scale. The intriguing nature of the interface structure is manifested by the presence of transition layers at the interface, which contain Si atoms in intermediate oxidation states called ''suboxide'' states (Si^{1+}, Si^{2+}, and Si^{3+}).[4–6] Although quite a few structural models of the transition layers have been proposed for SiO_2/Si(100) and SiO_2/Si(111) interfaces,[5–9] there are contradicting conclusions on the chemical abruptness of the interface and the thickness of the transition layers. These debates are directly related to the depth distribution of suboxide components in the interfacial region.

A very powerful and unique experimental tool to approach the issue of the chemical structure of the SiO_2/Si interface is a photoemission study of Si 2*p* core levels shifted chemically for the suboxide species (Si^{1+}, Si^{2+}, and Si^{3+}). In particular, the polar-angle dependence of the angle-resolved Si 2*p* intensities can be a useful technique to investigate the depth profiles of the individual oxidation states. Indeed, such a polar-angle-scan Si 2*p* study on a SiO_2/Si(111) interface was recently reported.[10] This study concluded upon a chemically abrupt interface model, in contradiction to the earlier ''graded interface model.'' [15] In this model the suboxide species are confined within interface layers composed of two possible interface terminations: interbilayer and intrabilayer terminations.[10] The study of Ref. 10 was not confirmed thereafter, and moreover there has been no such study on the chemical structure of the SiO_2/Si(100) interface.

The SiO_2/Si(100) interface is far more important for device applications and far more suitable for a theoretical investigation than the Si(111) counterpart. Indeed, extensive theoretical studies were recently performed for the SiO_2/Si(100) interface: while one suggested a chemically graded interface with the suboxide (Si^{1+}, Si^{2+}, or Si^{3+}) distributed over a range of 20 Å,[11] others introduced a very thin interface of 4 Å thickness (two or three transition layers) with different suboxide distributions.[12] This situation obviously requests an urgent experimental study on the chemical and atomic structure of the SiO_2/Si(100) interface.

In the present study, we measured the Si 2*p* core-level shifts of the various oxidation states (Si^{1+}, Si^{2+}, Si^{3+}, and Si^{4+}) for an ultrathin SiO_2/Si(100) interface using high-resolution angle-resolved photoemission. The SiO_2/Si(100) interface was formed by standard dry oxidation, and its thickness is estimated to be 6 Å, as explained below. We have investigated the depth distribution of the individual oxi-

dation states by measuring the intensities of the different Si $2p$ components as functions of the polar emission angle. These experimental data are quantitatively analyzed with a simple electron attenuation scheme. We clearly conclude on the existence of a chemically nonabrupt interface with the Si^{1+} and Si^{2+} species localized in the first interface layer, with the Si^{3+} species mostly in the second and third layers.

II. EXPERIMENTS

Angle-resolved photoemission experiments were performed on the high-resolution photoemission beam-line BL-1C of Photon Factory in KEK, Japan. This beam line is equipped with a commercial angle-resolved photoelectron spectroscopy system with a hemispherical electron analyzer (ARUPS-10, VG) mounted on a double-axis goniometer. The ultrathin SiO_2 film studied here was grown *in situ* by exposing a clean Si(100)2 $\times$1 substrate held at 600 °C to highly pure O_2 gas at a pressure of 5×10^{-8} torr for 3000 sec (150 L in total). The total thickness of the oxide layer is estimated to be 6 Å, as described below. The total-energy resolution was set to 70 meV at a photon energy of 130 eV and the angular resolution to 2° for all measurements. The angle-resolved Si $2p$ photoemission spectra were measured by changing the polar emission angle (θ) from 0° to 70°, with steps of 2.5°.

III. RESULTS AND DISCUSSION

Figure 1 shows high-resolution angle-resolved Si $2p$ spectra of SiO_2/Si(100) (150 L at 600 °C) taken at (a) $\theta=0°$ and (b) $\theta=60°$. For quantitative analyses all spectra were fitted by a standard curve-fitting procedure with spin-orbit doublets of Voigt functions.[13] The two spectra in Fig. 1 are normalized to have the same bulk peak (B) intensities. The intensity distribution and core-level shifts of the suboxide-oxide components and the overall line shapes are consistent to the previous reports (see Table I).[6–9] The core-level binding-energy shifts were determined accurately to be 1.00, 1.82, 2.62, and 3.67 eV for $Si^{1+}-Si^{4+}$, respectively. However, in contrast to the previous studies, two extra components (denoted α and β) were required to obtain reasonably good fits, which are located at low- and high-binding-energy tails of the bulk peak B, with binding energy shifts of -0.25 and 0.20 eV, respectively. That is, the Si substrate contribution cannot simply be fitted with a single component. Although the α and β components are minor in their intensities, they are consistently observed in all other samples formed at various different conditions with different oxide thickness.[13] We tentatively assume these components to be due to strained interfacial Si atoms without any Si-O bonds but a detailed discussion of them will be given separately. While α has practically no interference with the study of the suboxides, β has an overlap with the Si^{1+} component, affecting the intensity analysis for Si^{1+}. This point will be discussed more carefully below.

In order to extract the depth distribution of each suboxide component, the angle-resolved Si $2p$ spectra were taken by changing the polar angle θ, that is, by changing the probing depth by an overall $\cos\theta$ factor. Each θ-dependent Si $2p$ spectrum was then fitted like those in Fig. 1. In summary of this set of spectra, Fig. 2(a) shows the θ dependence of the intensities of the individual oxidation states (I_{x+}) normalized by the total intensities of the substrate-related components $I_{Si}=I_B+I_\alpha+I_\beta$. The symbols represent experimental data, and the curves are results of the simulation based on a simple interface model discussed below. As θ increases, going from normal emission to grazing emission, the normalized intensities for all four components increase monotonically but, very importantly, at certainly different rates. As

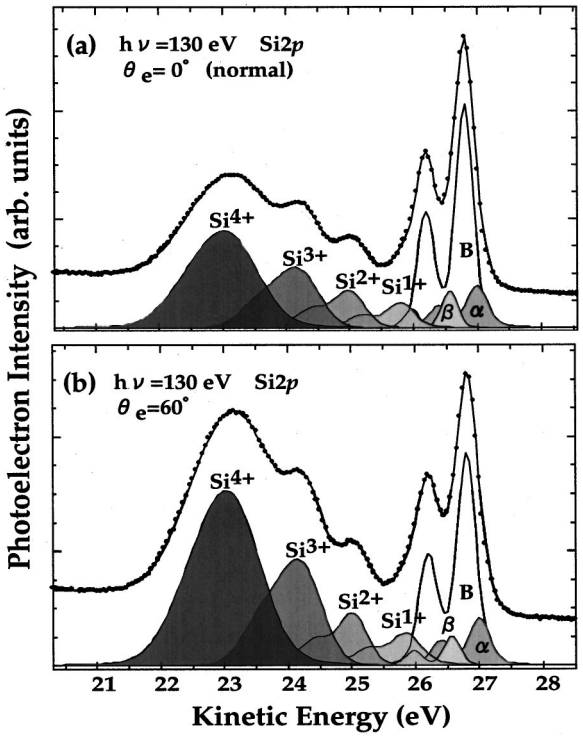

FIG. 1. Si $2p$ core-level spectra taken from ultrathin SiO_2/Si(100) at (a) polar emission angles θ of 0° and (b) 60°, with a photon energy ($h\nu$) of 130 eV. The ultrathin SiO_2 layer is formed by a 150-L O_2 dose on the Si(001)2$\times$1 surface, held at 600 °C. The dots are experimental data points, and the solid lines are the results of the curve fittings with the decompositions shown below.

TABLE I. Fitting parameters for the series of Si $2p$ core-level spectra shown partly in Fig. 1.

Fitting parameter	Optimized value
Spin-orbit splitting	0.61 eV
Branching ratio	0.5 eV
Lorentzian width	0.08 eV
Si^{1+} shift	1.00 eV
Si^{2+} shift	1.82 eV
Si^{3+} shift	2.62 eV
Si^{4+} shift	3.67 eV
α shift	-0.25 eV
β shift	0.20 eV
Bulk Gaussian width	0.28 eV

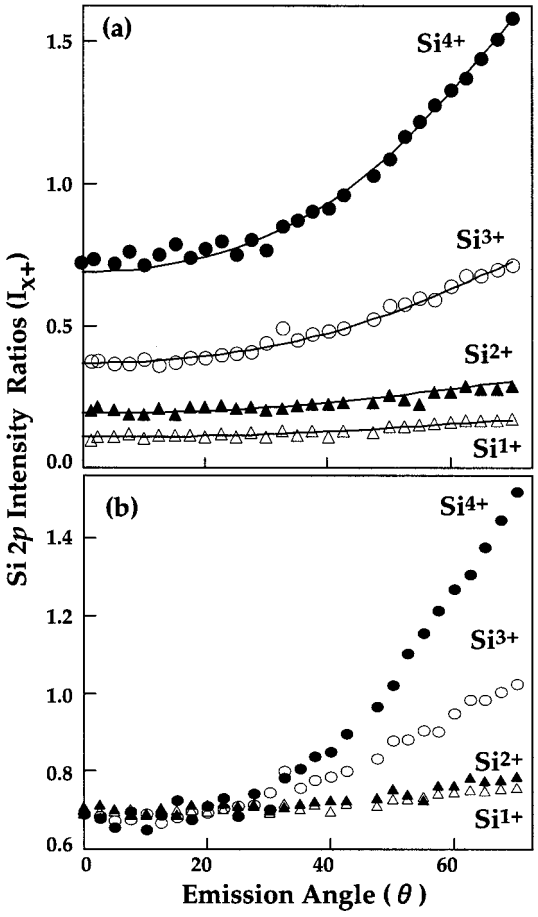

FIG. 2. (a) Intensity ratios of the Si $2p$ Si^{+}-Si^{4+} components to the total intensity of the Si substrate-related components as a function of the polar emission angle (θ). The symbols represent experimental data, and the curves the results of fitting based on the interface structure model explained in the text. (b) The same intensity ratios as in (a), but renormalized by the intensity at normal emission. This plot manifests itself in the different polar angle dependences of each suboxide component.

obvious from the renormalized data shown in Fig. 2(b), while the θ dependences of Si^{1+} and Si^{2+} are identical within the experimental uncertainty, Si^{3+} shows an apparently greater rate of increase. The increase of the Si^{4+} component is the steepest, which is naturally expected from the fact that the SiO_2 layers are on top of the suboxide layers, which makes the Si^{4+} component stronger in a more surface sensitive condition of a larger θ. Then the trend of different θ dependences of Si^{1+}/Si^{2+} and Si^{3+} suggests (i) that *the* Si^{1+} *and* Si^{2+} *species have the same depth distribution*, most probably at the first few interfacial layers (but with different population as suggested by their intensity difference), and (ii) that *the* Si^{3+} *species are distributed in a wider region* from the interface boundary toward the surface.

The intensity ratio of Si^{1+} to Si^{2+} is almost constant over the whole region of θ measured as 1.8. This indicates that the Si^{2+} species is approximately twice as ''popular'' as Si^{1+}. Quantitatively speaking, this population ratio should be taken with care, since the intensity of the Si^{1+} component can be affected by the presence of β (Fig. 1), whose origin is not firmly established, as mentioned above. When we fit the spectra without the β component, sacrificing the goodness of the fits, we obtain a population ratio between Si^{1+} and Si^{2+} of 1.5 instead of 1.8. However, the θ dependence of the intensities of these components given above is independent of the way of fitting concerning the β component.

A similar behavior of the Si $2p$ intensities for the Si^{1+}, Si^{2+}, and Si^{3+} species was recently observed in Ref. 10 for the ultrathin SiO_2/Si(111) interface. The authors of Ref. 10 also noted that the Si^{3+} species is distributed over a wider region of the interface than Si^{1+} or Si^{2+}, from the steeper increase of the intensity of Si^{3+}. However, an abrupt interface model was introduced for SiO_2/Si(111) based on the idea of statistical bond connection.[10] In this model, Si^{1+} and Si^{2+} are confined to the atomic layer just below the interface boundary, while Si^{3+} can be on *either* side of this boundary (i.e., in two different layers) with all interface bonds connected to Si or O statistically. This fact is crucial in explaining the stiffer θ dependence of Si^{3+} than Si^{1+} or Si^{2+}. However, if one applies such a simple bond connection to the case of the SiO_2/Si(100) interface, one can easily find that Si^{3+} (Si^{1+} or Si^{2+}) is confined within the layer just above (below) the interface boundary. This is because the ideal Si(100) interface layer has a unique termination with an interface Si atom, possessing only two broken bonds, which can only be in either Si^{1+} or Si^{2+} configurations. That is, the abrupt SiO_2/Si(100) interface has each suboxide component confined in a single atomic layer, in sharp contrast to the Si(111) case. The straightforward consequence of this fundamental difference of the local interfacial registry is that one cannot explain the stiffer θ dependence of the Si^{3+} species, or even the existence of Si^{3+} itself, in the abrupt interface model. Moreover, within the statistical bond connection, the populations of Si^{1+} and Si^{2+} should be the same for the SiO_2/Si(100) interface. This is clearly denied by the experimental observation given in Fig. 2.

It is thus obvious that the simple bond-connection model and the ideal abrupt interface are not compatible with the present experimental observation. In order to explain the θ dependence in Fig. 2 quantitatively, we constructed a simple nonabrupt, graded interface model as shown in Fig. 3. In this model, the concentration of impurities, such as H, F, and OH, are neglected, since the interface measured are formed by dry oxidation in ultrahigh vacuum at a very mild temperature. At the interface there might still be dangling-bond defects. However, the dangling-bond density is believed to be negligible on the order of 0.1 ML, which is the typical suboxide density under present discussion. As mentioned above, the first layer of the interface should consist only of Si^{1+} and Si^{2+} components. Taking into account of the intensity of Si^{2+}, which is 1.8 times larger than that for Si^{1+} at all emission angles, we set the population ratio for Si^{1+} and Si^{2+} at 1:1.8 (36% Si^{1+} and 64% Si^{2+} in the first interface layer). In order to account for the difference of the depth distribution between Si^{3+} and the other suboxides, the Si^{3+} species is put into more than two layers from the interface, i.e., at least in the second and third interface layers. Therefore, three transition layers are the minimum requirement to be consistent to the above experimental result. In more detail, there are two

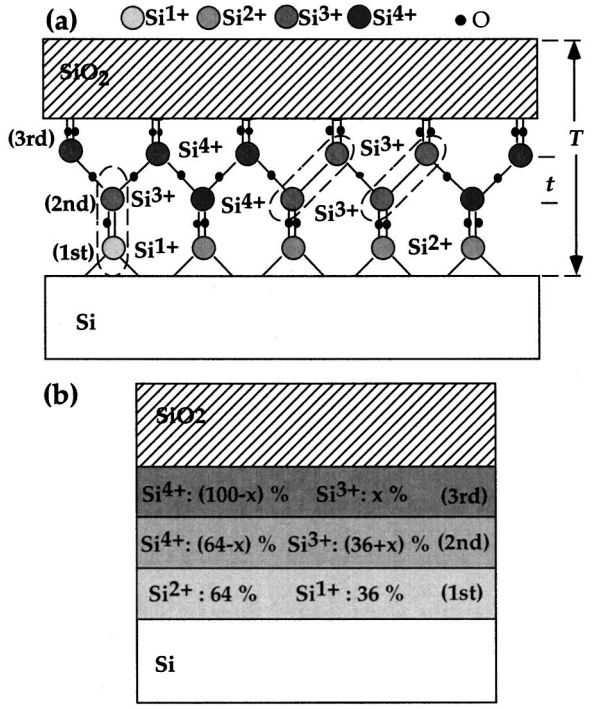

FIG. 3. (a) Side view of a simple chemically nonabrupt interface model for SiO_2/Si(100). See the text for a further explanation. Different suboxide species are depicted with different symbols, and the transition layers at the interface are composed of three chemically different layers. (b) Schematic illustration of the chemical composition of the transition layers based on the model shown in (a). The populations of suboxide components are given by *x*. The population of Si^{3+} in the third layer is explained in the text. The populations of the Si^{1+} and Si^{2+} species in the first transition layer are determined directly from the corresponding Si $2p$ component intensities.

kinds of Si^{3+} species at the second layer; one is bonded to the Si^{1+} species of the first layer, and the other is bonded to the Si^{3+} species of the third layer [see Fig. 3(a)]. Thus, with the population of Si^{3+} in the third layer (P_{3+}) of x%, there are $(100-x)$% Si^{4+} in the third layer and $(x+36)$% Si^{3+} and $(64-x)$% Si^{4+} in the second layer [Fig. 3(a)]. The parameter x is then treated as a fitting parameter in simulating the θ dependence.

The Si $2p$ intensity variation of each oxidation component (I_{x+}) can then be calculated using a simple electron damping scheme, which is similar to that of the previous report.[10] The intensity can be related to the population of each oxidation species at each transition layer (P_{x+}), as follows:

$$I_{x+}=N\times R_{x+}\times P_{x+}\times\exp\left(\frac{-D}{\lambda\cos\phi}\right).$$

Here $N(N=6.8\times10^{14}\ \mathrm{cm}^{-2})$ is the surface atomic density of a pure Si layer for Si(100), R_{x+} is the density ratio of Si in each oxidation state to that of bulk Si, P_{x+} is the population of each oxidation component in each transition layer, D is the thickness of the oxide-suboxide above the Si atoms emitting the photoelectrons, is λ the electron mean free path, and ϕ is the polar angle of emission within the crystal. Due to the inner potential, the internal emission angle ϕ and the external emission θ angle are not the same, and are related to each other by[14]

$$\sin\phi=\left(\frac{E_k}{E_k+V_0}\right)^{1/2}\sin\theta,$$

where V_0 is the inner potential set at 15.3 eV (Ref. 10) and E_k is the kinetic energy of the photoelectrons in vacuum.[15]

The mean free path can slightly be different between Si, SiO_x, and SiO_2, but this difference is neglected tentatively. The thickness D above the emitter is expressed by the thickness of a single atomic layer t (1.37 Å) for Si(100) and the total thickness of the suboxide-oxide layers T: for example, for the first layer just above the interface plane, $D=T-t$ [see Fig. 3(a)]. $R_{x+}(<1)$, the density ratio of Si in each oxidation state to that of bulk Si, is introduced to account for the variation of the Si density in the transition layers, for which no reliable experimental or theoretical values are available. The SiO_2 lattice has a density of Si atoms, which is 2.2 times smaller than that of pure Si. These two largely different densities should be matched at the transition layers, and this issue is directly related to the interface structure. In this work, we treat the density ratio of Si (R_{x+}) as another fitting parameter, with the constraint that $R_{1+}=R_{2+}$, since the Si^{1+} and Si^{2+} species are thought to be confined within the first interface layer, as mentioned above. Then, the resulting equations for the Si $2p$ intensity of each oxidation state are

$$I_{1+}=N\times R_{1+}\times\left(\frac{36}{100}\right)\times\exp\left(\frac{-T}{\lambda\cos\phi}\right),$$

$$I_{2+}=N\times R_{2+}\times\left(\frac{64}{100}\right)\times\exp\left(-\frac{T}{\lambda\cos\phi}\right),$$

$$I_{3+}=N\times R_{3+}\times\left[\left(\frac{36+x}{100}\right)\times\exp\left(\frac{-T+t}{\lambda\cos\phi}\right)+\left(\frac{x}{100}\right)\times\exp\left(\frac{-T+2t}{\lambda\cos\phi}\right)\right],$$

$$I_{4+}=N\times R_{4+}\times\left[\left(\frac{64-x}{100}\right)\times\exp\left(\frac{-T+t}{\lambda\cos\phi}\right)+\left(\frac{100-x}{100}\right)\times\exp\left(\frac{-T+2t}{\lambda\cos\phi}\right)+\exp\left(\frac{-T+t}{\lambda\cos\phi}\right)\right],$$

$$I_{\mathrm{Si}}=N\times\exp\left(\frac{-T}{\lambda\cos\phi}\right)\times\left[\frac{1}{\exp\left(\frac{t}{\lambda\cos\phi}\right)-1}\right].$$

The solid lines shown in Fig. 2 are obtained by fitting the experimental data with the parameters of R_1 $(=R_2)$, R_3, x, λ, and T, whose optimized values are given in Table II. The obtained values for the mean free path λ and the total oxide thickness T are consistent to the previous report on the SiO_2/Si(111) system. The optimized distribution of the sub-

TABLE II. Optimized parameters for the fitting of the θ dependence of the Si $2p$ component intensities for suboxide and oxide species based on the interface model given in Fig. 3, and the photoelectron damping scheme given in the text. The finalized results of the fits are compared to experimental data in Fig. 1(a).

Fitting parameter	Optimized value
Density ratio of Si for Si^{x+}; R_{x+}	
R_{1+}	0.83 ± 0.05
R_{2+}	0.83 ± 0.05 (same as R_{1+})
R_{3+}	0.63 ± 0.02
R_{4+}	0.46 (fixed)
Electron mean free path, λ	4.40 ± 0.05
Population of Si^{3+} in the third layer, x	$35.0 \pm 1.5\%$
Total thickness of oxide layer, T	5.7 ± 0.6

oxides and oxide at each transition layers are, 36% Si^{1+} and 64% Si^{2+}, 71% Si^{3+} and 29% Si^{4+}, and 35% Si^{3+} and 65% Si^{4+}, at the first, second, and third interfacial layers from the Si substrate, respectively [see Table II and Fig. 3(b)]. It can be found that the above model yields a fairly good agreement with the experimental results, reproducing the distribution of each suboxide peak very well (Fig. 2).

In the pioneering Si $2p$ study by Himpsel *et al.*,[5] the observation of the suboxide species led to two graded interface models. One of these models was originally proposed by Ohdomari *et al.*, with two interfacial layers of Si^{1+} and Si^{2+} (the first layer) and one of Si^{3+} (the second, upper, layer), respectively.[16] This graded interface model was motivated by the desire to solve the density mismatch between Si and SiO_2 mentioned above.[16] The density matching at the interface through transition layers is reflected in our simulation through the gradually varying suboxide density R_{x+} (Table II). The other model is composed of three interfacial layers of Si^{2+} (the first layer), Si^{1+} (the second layer), and Si^{3+} (the third, uppermost, layer), respectively, and of one dangling bond per each Si^{1+} atom.[5] The major difference between these two models and the present model lies in the distribution of the Si^{3+} species. In order to confirm our conclusion further, we also attempted simulations based on models with Si^{3+} species located within a single layer as in the two previous models. However, models with a single Si^{3+} layer cannot reproduce the θ dependence of the Si^{3+} component, which is steeper than that for Si^{1+} and Si^{2+} (Fig. 2), which is the most important aspect of the present experimental observation. Furthermore, as mentioned above, models with a single Si^{3+} layer cannot satisfy the complete bond connection, leaving a large number of dangling bonds.

Recently, two extensive theoretical calculations seemed to reach a general consensus on the ideal SiO_2/Si(001) interface structures, where the interface is composed of a single full monolayer of the Si^{2+} species.[17,18] The authors also noted that their ideal interface models cannot explain the suboxide species observed by photoemission. Their suggestions for more realistic graded interfaces were, however, different. Tu and Tersoff suggested a graded interface model with the first interface layer of the Si^{1+} species, and the second layer of Si^{2+} and Si^{3+}.[17] The nominal population ratio of the Si^{1+}, Si^{2+}, and Si^{3+} species was suggested to be 1:2:1. On the other hand, the authors of Ref. 18 introduced a model whose first interface layer is one of the Si^{1+} and Si^{2+} species, and whose second layer is one of Si^{3+} species. In this case the nominal density ratio of the Si^{1+}, Si^{2+}, and Si^{3+} species was 1:1:1. These two models are in contrast to the present interface model both qualitatively and quantitatively. Moreover, they cannot reproduce the steeper θ dependence of the Si^{3+} component, since at least two layers with Si^{3+} is necessary to be compatible with the present result.

On the other hand, for thicker SiO_2 films on Si(001) a recent molecular-dynamics simulation indicated a highly graded interface with a sequential distribution of Si^{1+}, Si^{2+}, and Si^{3+} species from the interfaces.[11] This model has transition layers of a thickness as large as $\sim$20 Å. The present result also denies this model, since Si^{1+} and Si^{2+} species are shown to be distributed in the same interfacial layer, and the extent of the interface is much smaller than this calculation. The latter discrepancy may come from the fact that the present experiment was done on an extremely thin SiO_2 layer. Another molecular-dynamics simulation for an ultrathin oxide on Si(001) yielded yet another interface model composed of three interfacial layers with Si^{1+} distributed over all three layers, with a Si^{2+} species only in the middle layer.[12] It is obvious that this model is also not compatible with the present result. It would be interesting to investigate the dependence of the interface structure on the total oxide thickness.

Finally we note that the present result is not expected to depend strongly on the conditions of the SiO_2 formation, such as the temperature and the O_2 pressure. This is because the suboxide distribution in the Si $2p$ photoemission has been established to be qualitatively invariant over a wide range of differently prepared SiO_2/Si(001) interfaces.[2,5,19–21]

IV. SUMMARY

We have investigated the structure and chemical abruptness of the SiO_2/Si(001) interface by measuring the polar-emission-angle dependence of the Si $2p$ suboxide components with high-resolution angle-resolved photoemission. It is shown that the polar-emission-angle dependences of the Si^{1+} and Si^{2+} components are identical, but this is in contrast to that of the Si^{3+} component: the Si^{3+} component exhibits a significantly steeper increase upon approaching the grazing emission. This leads to the conclusion that the Si^{3+} species has a wider depth distribution than Si^{1+} and Si^{2+}. The angular dependence of each suboxide component is quantitatively analyzed based on a simple interface model, assuming that all the bonds are connected. From this analysis, it is concluded that the Si^{1+} and Si^{2+} species exist just at the first interface layer, while the Si^{3+} species is distributed over the second and third layers from the interface. This model can successfully and quantitatively describe the experimental data through a simple electron damping scheme. The present result thus clearly indicates a chemically nonabrupt interface, in contrast to most of the recent interface structure models

proposed by elaborate theoretical calculations. This is also in contrast to the recent abrupt interface model for the SiO_2/Si(111) interface derived from a similar experimental study.

ACKNOWLEDGMENTS

This work was supported by STARC Grant No. (99-02) from Semiconductor Technology Academic Research Grant-in-Aid for Scientific Research (B2-10555100) from the Ministry of Education, Science, and Culture of Japan. This work was done under Special Project No. 97S1-002 at the Institute of Material Structure Science in KEK. H.W.Y. was supported by the Atomic-Scale Surface Science Research Center funded by KOSEF, the Brain Korea 21 program of the Ministry of Education, and the Tera-level Nanodevices program (21 century Frontier Programs).

*Author to whom correspondence should be addressed: FAX: 82-2-312-7090; Email address: yeom@phya.yonsei.ac.kr

[1] E. Hasegawa, A. Ishitani, K. Akimoto, M. Tsukiji, and N. Ohta, J. Electrochem. Soc. **124**, 273 (1995).
[2] S. Iwata and A. Ishizaka, J. Appl. Phys. **79**, 6653 (1996).
[3] D. A. Muller, T. Sorsch, S. Moccio, F. H. Baumann, K. Evans-Lutterodt, and G. Timp, Nature (London) **399**, 758 (1999).
[4] G. Hollinger and F. J. Himpsel, Appl. Phys. Lett. **44**, 93 (1984).
[5] F. J. Himpsel, F. R. McFeely, A. Taleb-Ibrahimi, A. Yarmoff, and G. Hollinger, Phys. Rev. B **38**, 6084 (1988).
[6] K. Ohishi and T. Hattori, Jpn. J. Appl. Phys. **33**, L675 (1994).
[7] M. T. Sieger, D. A. Luh, T. Miller, and T.-C. Chiang, Phys. Rev. Lett. **77**, 2758 (1996).
[8] W. K. Choi, F. W. Poon, F. C. Lph, and K. L. Tan, J. Appl. Phys. **81**, 7386 (1997).
[9] H. Ono, T. Ikarashi, K. Ando, and T. Kitano, J. Appl. Phys. **84**, 6064 (1998).
[10] D.-A. Luh, T. Miller, and T.-C. Chiang, Phys. Rev. Lett. **79**, 3014 (1997).
[11] K.-O. Ng and D. Vanderbilt, Phys. Rev. B **59**, 10 132 (1999).
[12] Alexander A. Demkov and Otto F. Sankey, Phys. Rev. Lett. **83**, 2038 (1999).
[13] H. W. Yeom, H. Hamamatsu, T. Ohta, and R. I. G. Uhrberg, Phys. Rev. B **59**, R10 413 (1999).
[14] T. Miller, A. P. Shapiro, and T.-C. Chiang, Phys. Rev. B **31**, 7915 (1985).
[15] A. Ourmazd, D. W. Taylor, J. A. Rentschler, and J. Bevk, Phys. Rev. Lett. **59**, 213 (1987).
[16] I. Ohdomari, H. Akztsu, Y. Yamakoshi, and K. Kishimoto, J. Appl. Phys. **62**, 3571 (1987).
[17] Yuhai Tu and J. Tersoff, Phys. Rev. Lett. **84**, 4393 (2000).
[18] R. Buczko, S. J. Pennycook, and S. T. Pantelides, Phys. Rev. Lett. **84**, 943 (2000).
[19] M. Niwano, H. Katakura, Y. Takeda, Y. Takakuwa, N. Miyamoto, A. Hirawa, and K. Yagi, J. Vac. Sci. Technol. A **9**, 195 (1991).
[20] Y. Enta, Y. Miyanishi, H. Irimachi, M. Niwano, M. Suemistu, N. Miyamoto, E. Shigemasa, and H. Kato, Phys. Rev. B **57**, 6294 (1998).
[21] Z. H. Lu, S. P. Tay, T. Miller, and T. C. Chiang, J. Appl. Phys. **77**, 4110 (1995).